Supporting Information Notes S1−S4 and Figs. S1−S4

Deviation from symmetrically self-similar branching in trees predicts altered hydraulics, mechanics, light interception and metabolic scaling

Duncan D. Smith[1,*], John S. Sperry[1], Brian J. Enquist[2], Van M. Savage[3], Katherine A. McCulloh[4], Lisa P. Bentley[2]

[1]Department of Biology, University of Utah, Salt Lake City, UT, 84112, USA
[2]Department of Ecology and Evolutionary Biology, University of Arizona, Tucson, AZ, 85721, USA
[3]Department of Biomathematics, University of California, Los Angeles, CA, 90095, USA
[4]Department of Forest Ecosystems and Society, Oregon State University, Corvallis, OR, 97331, USA

[*]Corresponding author: duncan.smith@utah.edu; 801-585-0381

Notes S1 Materials used in P_f measurements

Trees and shrubs used for empirical P_f measurements came from three locations within the United States. All networks came from healthy looking plants with minimal dieback. All species were either native or naturalized and harvested from natural settings.

Red Butte Canyon (RBC; 40.8° N, 111.8° W) is located adjacent to the University of Utah in Salt Lake City, UT. One *Quercus gambelii* and one *Acer grandidentatum* were collected in the spring of 2008 while others from the area were collected during the late winter and spring of 2010. Only *Cornus sericea*, *Rhus glabrum*, and *Salix exigua* were located near permanent surface water. Self-supporting networks were preferred although shrubby *Rhus trilobata* was more prostrate and clonal *Salix exigua* likely leaned against neighbors. Plants overshadowed by neighbors were avoided but many had similar sized neighbors nearby.

Cedar Creek (CC; 45.4° N, 93.2° W) is part of the eastern deciduous forest located *ca.* 45 km north of Minneapolis, MN. Plants were collected in 2008 from sites without permanent surface water and soils ranging from very wet to sandy and drier. All plants were self-supporting and received direct sun for at least half of the daytime.

The *Pinus ponderosa* trees came from the Coronado National Forest (CNF) near Tucson, AZ during February 2007. The trees chosen were relatively isolated from neighbors.

Notes S2 WBE compatibility with $L^*_\uparrow(D)$ function (Eqn. 8)

The WBE model achieves an eventual 2/3-power $L^*_\uparrow$ by D relationship by scaling individual lengths with $D^{2/3}$ and summing those lengths. The form of this relationship conforms to

$$L^*_\uparrow = aD^{2/3} - l_o \tag{S1}$$

which is given by McMahon & Kronauer (1976) to apply to all trees regardless of their branching architecture. We use Eqn. S1 as a starting point and show how it is entirely consistent with the special case of WBE architecture when the correct l_o is used. We derive this WBE-compatible l_o and use it in Eqn. S1 for application to all modeled trees (see Eqn. 8 in main text). We do this in order to be able to compare the properties of WBE and non-WBE trees.

In the special case of WBE structure, segment lengths, l, scale with their diameters to the 2/3 power:

$$l = cD^{2/3}. \tag{S2}$$

Twig length, l_t, may be calculated independently both by Eqn. S2 and as $L^*_\uparrow(D_t)$ (Eqn. 10 in the main text). Therefore,

$$l_t = L^*_\uparrow(D_t) = aD_t^{2/3} - l_o = cD_t^{2/3} \tag{S3}$$

making,

$$l_o = D_t^{2/3}(c - a) \tag{S4}$$

As a is already defined by safety from buckling, finding l_o requires a value of c that satisfies WBE.

In the WBE architecture, symmetric self-similarity produces levels of identical branch segments. Using WBE terminology, k is the level index where the trunk is level $k = 0$ and the twigs comprise level $k = N$. The diameter and length ratios between segments in adjacent levels are β and γ.

$$\beta \equiv \frac{D_{k+1}}{D_k} = f^{-1/2} \tag{S5}$$

$$\gamma \equiv \frac{l_{k+1}}{l_k} = f^{-1/3} \tag{S6}$$

The second equalities only apply to WBE structures. Using the twig level as a reference in Eqn. S6, it follows that $l_N/l_{N-1} = f^{-1/3}$. Then, applying Eqn. S4 to Eqn. S1 and using Eqns. 9-10 to get segment lengths gives

$$\frac{l_N}{l_{N-1}} = \frac{aD_t^{2/3} - l_o}{(aD_{N-1}^{2/3} - l_o) - (aD_t^{2/3} - l_o)} = \frac{aD_t^{2/3} - (c-a)D_t^{2/3}}{aD_{N-1}^{2/3} - aD_t^{2/3}}. \tag{S7}$$

Based on Eqn. S5, the D of any level k may be defined using D_N $(= D_t)$ as

$$D_k = D_N f^{(N-k)/2} \tag{S8}$$

With $k = N - 1$, plugging Eqn. S8 into Eqn. S7 produces

$$\frac{l_N}{l_{N-1}} = \frac{aD_N^{2/3} - (c-a)D_N^{2/3}}{aD_N^{2/3} f^{1/3} - aD_N^{2/3}} = \frac{2a-c}{af^{1/3} - a} \tag{S9}$$

Recalling the requirement that $l_N/l_{N-1} = f^{-1/3}$, we get

$$c = a(1 - f^{1/3}) \tag{S10}$$

and plugging Eqn. S10 into Eqn. S4 finally gives

$$l_o = af^{-1/3}D_t^{2/3}. \tag{S11}$$

Equation S11 provides an l_o which satisfies $\gamma = f^{-1/3}$ at the twig level in WBE trees when plugged into Eqn. S1. The resulting equation (Eqn. 8 in the main text) was then used for all trees, regardless of structure.

However, the preceding equations only explicitly show that the length ratio between twigs and their mothers complies to WBE. We must additionally check the length ratio between all other adjacent levels by applying Eqn. S4 to Eqn. S1 and using Eqn. 9 to get segment lengths:

$$\frac{l_{k+1}}{l_k} = \frac{(aD_{k+1}^{2/3} - l_o) - (aD_{k+2}^{2/3} - l_o)}{(aD_k^{2/3} - l_o) - (aD_{k+1}^{2/3} - l_o)} = \frac{aD_{k+1}^{2/3} - aD_{k+2}^{2/3}}{aD_k^{2/3} - aD_{k+1}^{2/3}}. \tag{S12}$$

Substituting diameters from Eqn. S8 into Eqn. S12 produces

$$\frac{l_{k+1}}{l_k} = \frac{aD_N^{2/3}f^{(N-k-1)/3} - aD_N^{2/3}f^{(N-k-2)/3}}{aD_N^{2/3}f^{(N-k)/3} - aD_N^{2/3}f^{(N-k-1)/3}} = f^{-1/3} \tag{S13}$$

which meets the WBE requirement. Note that all l_o values canceled out in Eqn. S12. Therefore, in a WBE tree, across all levels except the twig level, any value of l_o in Eqn. S1 satisfies the WBE length ratio requirement. However, a specific l_o (Eqn. S11) is needed to make the twig level comply. In the strict rules of WBE architecture, l_o is a function of f, which is a constant. We used $f = 2$ to obtain the generic l_o for use in all trees. In non-WBE trees, branching only needs to follow Eqn. S1 where l_o can be set to any value. Because l_o only influences twig length (Eqn. S12), the only real consequence of using $f = 2$ for all trees is that symmetrically branching trees with $f > 2$ have twigs which are slightly shorter than WBE would predict.

Notes S3 Branch segment hydraulic conductance

As stated in the main text, we follow the Sperry *et al.* (2012) model of xylem architecture to determine hydraulic conductance of each branch segment. To summarize, their model takes branch diameter as an input and a number of equations are used to define the dimensions and numbers of functional conduits in that branch. Incorporating conduit length (= branch segment length) allows hydraulic conductance to be calculated with the Hagen-Poiseuille equation. In general, we utilize the default coefficients given by Sperry *et al.*. The equations used are as follows.

Conduit diameters, D_c (μm), increase with stem diameter, D (mm). This taper occurs both within stems and across stems and is given by

$$D_c = a_{tap} D^{b_{tap}}. \tag{S14}$$

The exponent, $b_{tap} = 1/3$, provides the optimal tapering defined by Savage *et al.* (2010) while the multiplier, $a_{tap} = 7.9$, corresponds with a maximum D_c of 10 μm in the default twig diameter, $D_t = 2$ mm.

The number of conduits per xylem area, N_c/A_x (mm^{-2}), tends to decrease as conduits become wider

$$N_c/A_x = a_{pak} D_c^{b_{pak}} \tag{S15}$$

The exponent, $b_{pak} = -2$, also comes from Savage *et al.* (2010) and it corresponds to a constant fraction of xylem area being occupied by conduits, regardless of their diameter. The multiplier, $a_{pak} = 10^5$ indicates that 10% of xylem area is occupied.

Part of the stem area is devoted to a pith in the center, which is given a constant diameter of 1 mm. On the outside of the stem is phloem, periderm, and possibly cortex. These are collectively the "bark" and bark thickness, T_{brk} (mm), increases with D as

$$T_{brk} = a_{brk} D^{b_{brk}} \tag{S16}$$

Parameters $b_{brk} = 1.05$ and $a_{brk} = 0.0225$ come from thin-barked *Acer grandidentatum*. The area between pith and bark is the total xylem area, ΣA_x. However, the oldest xylem near the pith eventually loses function and becomes heartwood with functional sapwood outside of it. Sapwood area, A_{sap}

(mm^2), increases with D but cannot exceed ΣA_x. Therefore,

$$A_{sap} = \begin{cases} a_{sap} D^{b_{sap}} & \text{if } a_{sap} D^{b_{sap}} < \Sigma A_x, \\ \Sigma A_x & \text{otherwise.} \end{cases} \tag{S17}$$

The parameters, $b_{sap} = 1.93$ and $a_{sap} = 0.905$, are also based on *A. grandidentatum* which is diffuse-porous with multiple years of functional xylem.

Equations S14−S17 collectively define the numbers and diameters of all functional conduits within a stem of any diameter. Using the Hagen-Poiseuille equation, one can then predict stem hydraulic conductivity. The Hagen-Poiseuille equation makes predictions for laminar flow through open, cylindrical tubes. We account for resistive endwalls in xylem with an angiosperm correction factor, $a_{ew} = 0.44$, meaning actual conductivity is 44% of that predicted by Hagen-Poiseuille (Hacke *et al.* 2006). For our model, we combined all of the above into a single integral that predicts branch segment hydraulic conductivity, κ (mm^4 MPa^{-1} s^{-1}):

$$\kappa = c_2 \left[\frac{x^{c_1}}{c_1} - \left(\frac{2a_{brk}(b_{brk}+1)x^{c_1+b_{brk}-1}}{c_1+b_{brk}-1} \right) + \left(\frac{4a_{brk}^2 b_{brk} x^{c_1+2b_{brk}-2}}{c_1+2b_{brk}-2} \right) \right] \Bigg|_{x=D_v}^{D} \tag{S18}$$

where

$$c_1 = 4b_{tap} + b_{tap}b_{pak} + 2,$$

$$c_2 = a_{ew}\left(\pi^2 a_{pak} a_{tap}^{b_{pak}+4}\right) / \left(256\mu 10^{12}\right),$$

and μ (MPa s) is the dynamic viscosity of water. The D_v is a “virtual” diameter. By way of explanation, note that Eqn. S14 predicts D_c at the bark-xylem interface (not at the stem surface). When integrating over the sapwood area, we recognize that the current heartwood-sapwood interface is where the bark-xylem interface was at one time. Therefore, in order to predict D_c at this location, we need to know what the overall stem diameter was at that time. That diameter is D_v, which must be found numerically. Branch segment hydraulic conductance (mm^3 MPa^{-1} s^{-1}) is just κ/l.

Notes S4 Partial derivation of $L_{crit}(D_T)$ function (Eqn. 13)

Based on Greenhill (1881), Jaouen *et al.* (2007) define L_{crit} as

$$L_{crit} = \frac{\pi^{1/2} E^{1/2} r_T^2 c(|m-4n+2|)}{4(M_{tot} g)^{1/2}}. \tag{S19}$$

The r_T is trunk radius, g is gravity and E is Young’s elastic modulus (N m^{-2}). Equation S19 is somewhat problematic as both M_{tot} and r_T are inputs which means L_{crit} is predicted for a constrained mass and trunk radius. We prefer that M_{tot} be a function of r_T and tree form. We express M_{tot} as a function of r_T by using tissue density, ρ, and volume, V, predicted using Eqn. 15 and $V_f = P_f$.

$$M_{tot} g = V\rho g = \pi r_T^2 L_{crit} P_f \rho_g \tag{S20}$$

We also combine ρ and g into ρ_g which is the specific weight of supporting tissue (N m^{-3}). The ratio of E/ρ_g is approximately constant across woody plants (125^3 m; Niklas 1994). Substituting Eqn. S20 into Eqn. S19, rearranging, and converting r_T to D_T leads to Eqn. 13 in the main text. To predict b in Eqn. 8, we used a WBE tree with 1024 twigs and $f^* = 2$. This tree resulted in $m = 2.91$ and $n = 0.96$. Among other WBE trees ($2^4 - 2^{12}$ twigs), larger size tended to increase both m (2.28 to 3.06) and n (0.64 to 1.03). However, the resulting b changed very little as size increased (range = 107.55 to 108.25). By comparison, a "fishbone" tree with 1024 twigs would have $b = 141.19$.

It should be noted that using parameters that correspond to a straight column ($P_f = 1$, $m = 1$ and $n = 0$) in Eqn. 13 produces

$$L_{crit}(D) = 0.788 \left(\frac{E}{\rho_g}\right)^{1/3} D^{2/3} \tag{S21}$$

which is essentially[1] the common equation used for critical heights (e.g. Niklas 1994).

References

Greenhill AG. 1881. Determination of the greatest height consistent with stability that a vertical pole or mast can be made, and of the greatest

[1]A constant of 0.792 instead of 0.788 is often cited but this apparently stems from Greenhill's (1881) imprecise estimation of the first positive root of the Bessel function. However, this 0.5% overestimation is likely of little consequence

height to which a tree of given proportions can grow. *Proceedings of the Cambridge Philosophical Society* **4**: 65–73.

Hacke UG, **Sperry JS**, **Wheeler JK**, **Castro L**. **2006**. Scaling of angiosperm xylem structure with safety and efficiency. *Tree Physiology* **26**: 689–701.

Jaouen G, **Alméras T**, **Coutand C**, **Fournier M**. **2007**. How to determine sapling buckling risk with only a few measurements. *American Journal of Botany* **94**: 1583–1593.

McMahon TA, **Kronauer RE**. **1976**. Tree structures: Deducing the principle of mechanical design. *Journal of Theoretical Biology* **59**: 443–466.

Niklas KJ. **1994**. The allometry of safety-factors for plant height. *American Journal of Botany* **81**: 345–351.

Olson ME, **Aguirre-Hernández R**, **Rosell JA**. **2009**. Universal foliage-stem scaling across environments and species in dicot trees: plasticity, biomechanics and Corner's Rules. *Ecology Letters* **12**: 210–219.

Savage VM, **Bentley LP**, **Enquist BJ**, **Sperry JS**, **Smith DD**, **Reich PB**, **von Allmen EI**. **2010**. Hydraulic trade-offs and space filling enable better predictions of vascular structure and function in plants. *Proceedings of the National Academy of Sciences of the United States of America* **107**: 22722–22727.

Sperry JS, **Smith DD**, **Savage VM**, **Enquist BJ**, **McCulloh KA**, **Reich PB**, **Bentley LP**, **von Allmen EI**. **2012**. A species' specific model of the hydraulic and metabolic allometry of trees I: model description, predictions across functional types, and implications for inter-specific scaling. *Functional Ecology* **26**: 1054–1065.

Figures

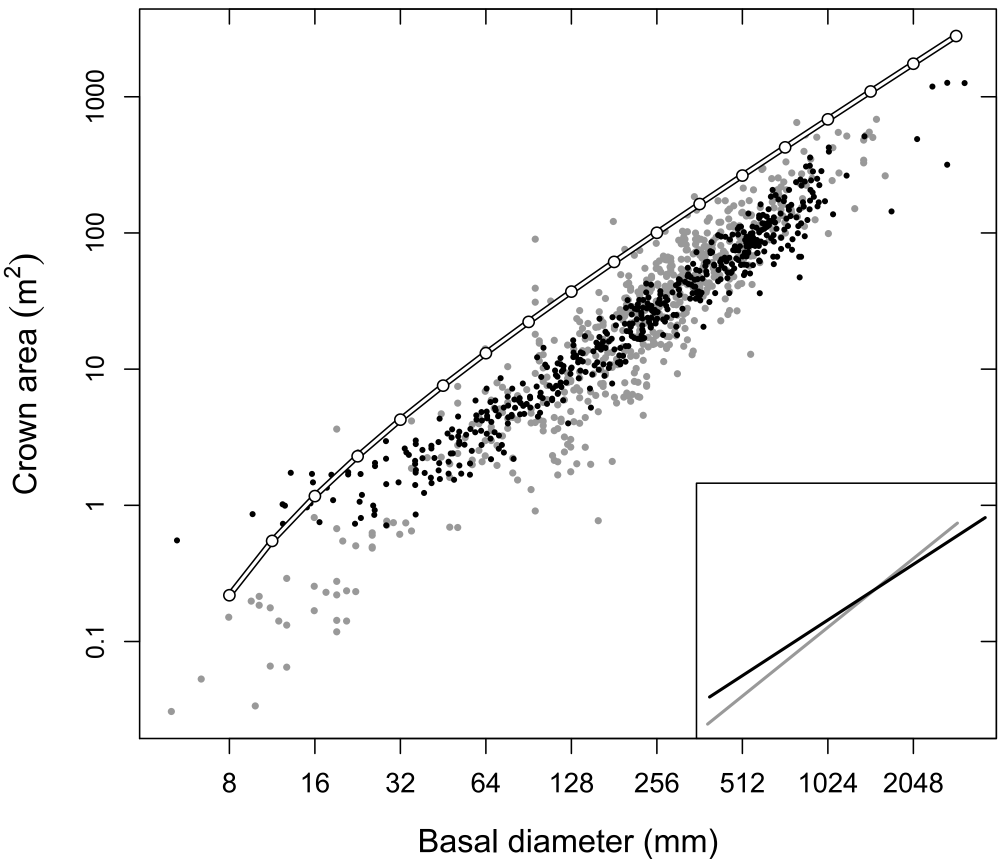

Figure S1: Measured and modeled crown area scaling. Closed circles indicate data from angiosperms (grey) and conifers (black). OLS regressions for these data (inset) had similar but significantly different slopes ($p < 0.01$). Random model trees (not shown) whose crown areas matched the angiosperm regression $\pm$ 5% were used to predict a P_f ontogeny (see Fig. 3). Open circles indicate WBE trees from the model. The model was built agnostic to the empirical crown area data. Therefore, it is somewhat surprising that not only did model trees fall among the data, but the WBE trees (which should have among the largest crowns for their trunk diameter) more or less followed the upper bound of the empirical data.

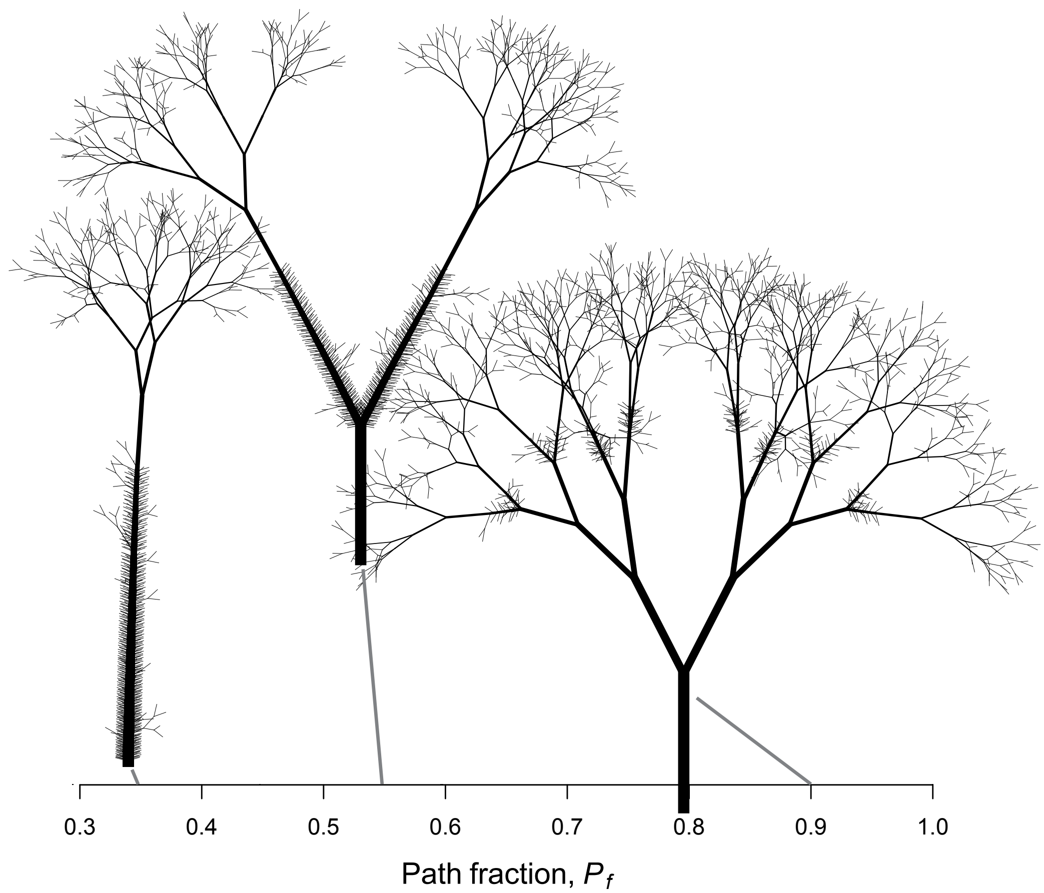

Figure S2: Three sample 1024-twig trees formed when more than one asymmetry parameter, u, is used in each tree. Such trees were excluded from the model due to their unrealistic nature.

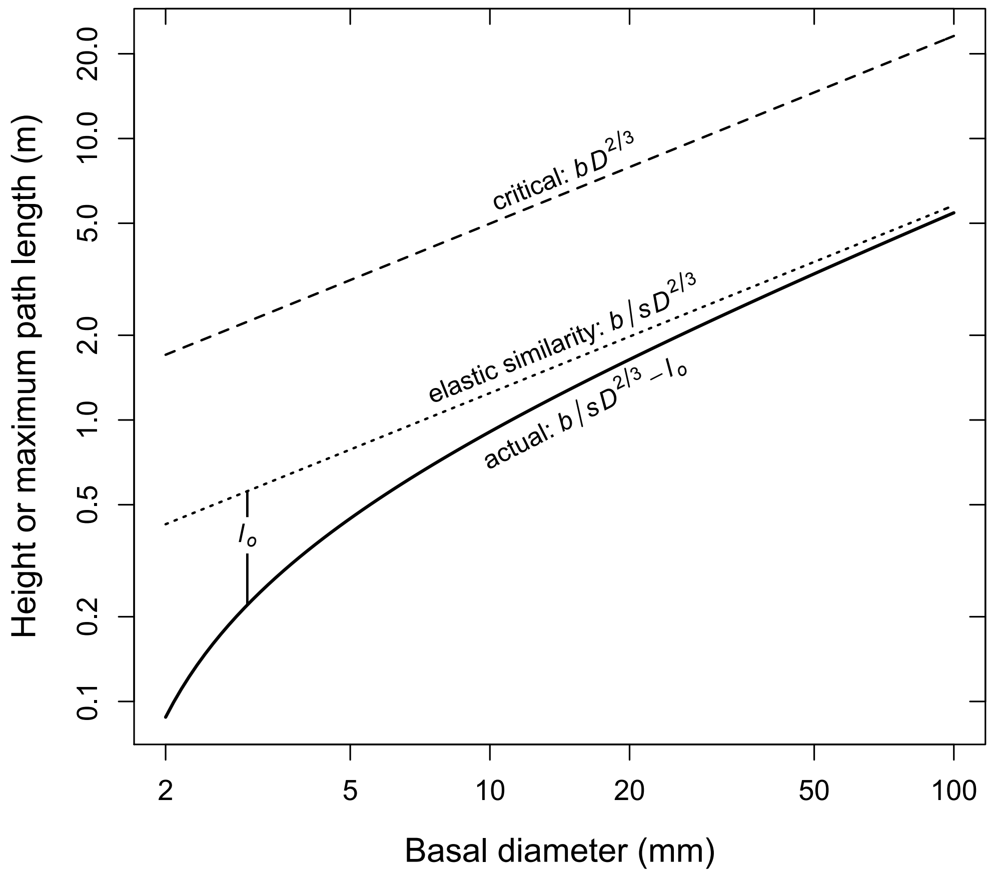

Figure S3: Illustration of the equations used to determine tree heights and path lengths. Plots use model inputs with an eventual safety factor of 4 and $D_t = 2$ mm. From top to bottom, the "critical" path (dashed; Eqn. 13) predicts the heights of WBE trees at elastic buckling. The "elastic similarity" path (dotted) parallels the critical line and thereby provides a constant safety factor from buckling. The "actual" path (solid; Eqn. 8) only approaches elastic similarity because of the constant virtual length, l_o, that exists because twigs do not taper to zero. Note that l_o is constant but does not appear so due to the log-log plotting axis.

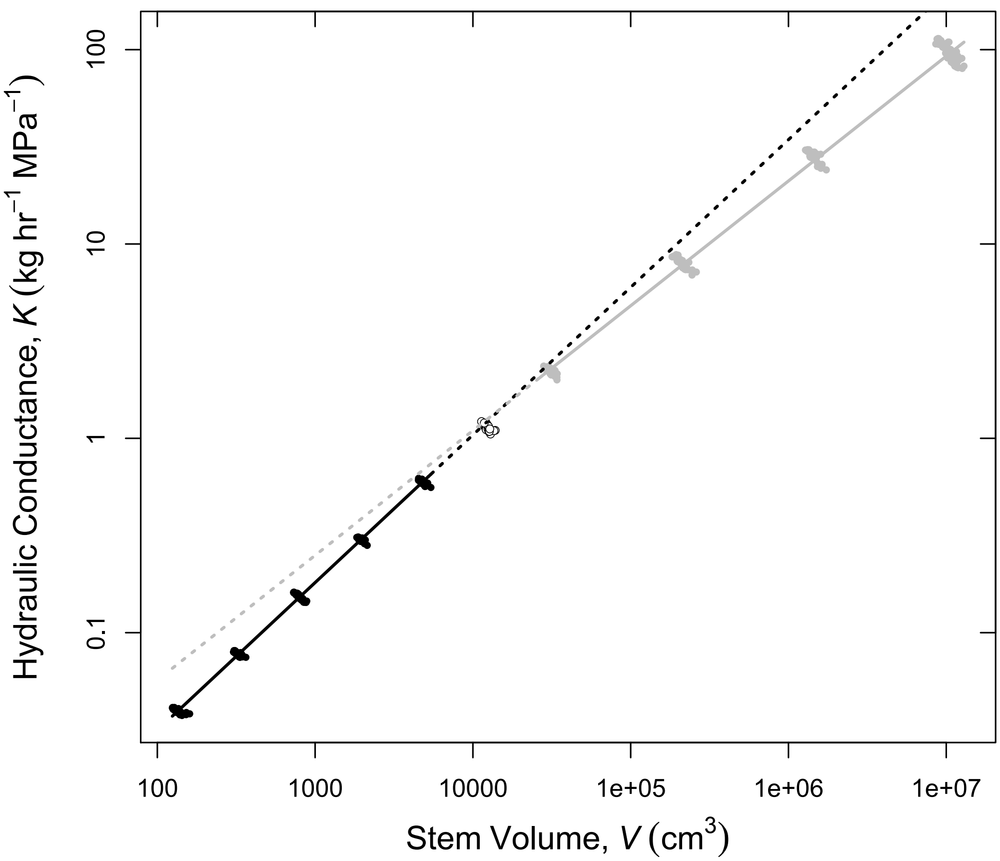

Figure S4: Metabolic scaling (i.e. $K \propto V^{cq}$) for trees which follow the crown area scaling measured by Olson *et al.* (2009; i.e. scenario three, S_3). The three colors correspond to P_f decreasing (black; $2^6 - 2^{10}$ twigs), P_f increasing (grey; $2^{12} - 2^{18}$ twigs) and trees in between (open; 2^{11} twigs; see Fig. 3, dashed line and Fig. 5, "S_3"). Solid SMA regression lines are extended by dotted lines to highlight the non-log-linearity caused by decreasing and then increasing P_f.